

Similarity and Scaling Effects in PEM Fuel Cells

A. M. Tahsini

Tehran, Iran

Abstract

The aim of the present study is to investigate similarity in the proton exchange membrane fuel cells and also to analyze the impacts of geometric scaling on the polarization curve. The effects of concentration distribution are analyzed and it is illustrated that both lateral and longitudinal variation of the species concentrations are important and effective on the polarization curve. Also the similarity is examined and it is concluded that the similarity may exist in fuel cells behavior considering the proper requirements, and also the effects of scaling on different regions of the polarization curve are studied. Here, the two-dimensional, single-phase, steady-state, isothermal, and multi-component system of flow fields governing equations are used besides the equations for electric and ionic potentials to simulate the fuel cell operation, where the cell-centered finite-volume method is utilized as a numerical scheme.

Keywords: Fuel cell; Numerical study; Polarization curve; Scaling; Similarity

Nomenclature

c_j	concentration of species j
D_{eff}	effective mass diffusion coefficient
e	specific internal energy
F	Faraday constant
h	specific enthalpy
I	total current density
j_{ref}	reference exchange current density
L_c	channel length
m_j	mass fraction of species j
p	pressure
R	universal gas constant
sc	scale factor
T	temperature
u	axial velocity
U_o	open circuit potential

V_c	working voltage
v	lateral velocity
x	coordinate across channel
y	coordinate along channel

Greek symbols

α	charge transfer coefficient
ε	porosity
$\eta_{a,c}$	anode and cathode over-potentials
κ	ionic conductivity
$\varphi_{e,p}$	electric and ionic potentials
ρ	density
σ	electric conductivity
$\dot{\omega}_j$	mass rate of production of species j

1. Introduction

Fuel cells directly convert chemical energy into electricity, and they require the continuous sources of oxidizer and fuel streams to sustain the chemical reactions. The first fuel cell was invented about 180 years ago, but the commercial use of fuel cells happened more than a century later in space programs of NASA. At the moment, they are widely being used in other applications, especially due to the fact that they are almost-zero-emission and low-noise devices with high energy efficiencies.

There is a focus on fuel cell engineering to achieve higher performance and durability, better startup characteristics, and cost reduction. Therefore, investigations and optimizations of different physicochemical processes in the fuel cells are strongly under consideration yet, and the surveys of scientific literature show that numerous researches have been carried out numerically and

experimentally in this area. Some of recent studies on proton exchange membrane fuel cells (PEMFC) are mentioned here briefly.

Gurau et al. [1] developed a two-dimensional (2-D) model to predict the polarization curve of the PEMFC using Navier Stokes equations by steady-state and single-phase assumptions. They analyzed the effect of some parameters such as cell temperature and inlet velocity on the polarization curve. Singh et al. [2] used similar model to predict the impacts of co-flow and counter-flow streams of fuel and oxidizer on the limiting current of the fuel cells. Dutta et al. [3] developed a single-phase and steady-state three-dimensional (3-D) mathematical model to simulate the straight channel PEMFCs and studied the effect of membrane thickness on the current density profiles. They also used this model to predict the temperature distribution in fuel cells [4].

Hsing and Futerko [5] predicted the dependence of water product leaving the anode on hydrogen and oxygen stoichiometries, current density, and cell temperature using 2-D model. Natarajan and Nguyen [6] developed a two-phase and transient 2-D model to study the dynamics of liquid water at the low and high current densities, and showed that the liquid water transport is the slowest mass-transfer phenomenon in the cathode of the PEMFCs. Wang et al. [7] performed similar study and illustrated the border between single- and two-phase regimes and its dependency on the air inlet velocity. You and Liu [8] used a two-phase model too, to study the effect of operating current density on the liquid saturation.

Chu et al. [9] investigated the effect of gas diffuser layer's porosity on the polarization curve using one-dimensional analysis. Burning and Djilali [10] studied the influence of working temperature and inlet pressure on the polarization curve of the PEMFCs by 3-D simulations. They also utilized this model to study the fuel cells with serpentine gas channel configurations [11]. Hu et al. [12] developed a two-phase 3-D model with the focus on the water content distribution in the PEM fuel cells. Hu et al. [13] studied numerically the polarization curve of fuel cells with interdigitated configurations.

Lum and McGuirk [14] investigated the effects of electrode thickness, oxidant concentration and channel length on fuel cell performance by 3-D analysis. Ying et al. [15] and Inoue et al. [16] analyzed the impacts of channel configuration on polarization curve of the PEMFCs. Lin et al. [17] performed the optimization procedure to seek the optimal combination of the design parameters, including the channel width ratio and the porosity. Yan et al. [18] proposed a tapered channel configuration to improve the efficiency of fuel utilization for PEMFCs.

Meng [19-21] developed a transient 3-D model to study the response of the fuel cell to a step change of the cell voltage. Secanell et al. [22] used a numerical optimization scheme in order to maximize the fuel cell current density at a given voltage with respect to the electrode's composition parameters. Shimpalee and Van Zee [23] investigated the impacts of channel geometry and flow direction, and Cheng et al. [24] studied the influence of geometric parameters and catalyst layer composition on the performance of PEMFCs.

Wu et al. [25] performed a numerical analysis of the dynamic performance of PEM fuel cells during startup or load change processes. Jang et al. [26] studied numerically the influences of the flow field configurations on the fuel utilization, water removal, and the cell performance of the PEMFCs. Gurau and Mann [27] presented an overview of the mathematical issues in the modeling of the multiphase transport in PEMFCs at a macroscopic scale. Min [28] used a two-phase 3-D model to study the water saturation distribution and cathode humidity effect on the cell

performance. Fontana et al. [29] investigated the influence of non-uniform cross-sectional area channel flow on the polarization curve.

Massonnat et al. [30] predicted the time-variation of voltage and temperature of the PEMFCs using 3-D numerical simulations. Mancusi et al. [31] investigated the time variation of two-phase flow patterns in the gas channel with tapered configuration. Chaudhary et al. [32] used a computational procedure to predict temporal variation of membrane water content and water saturation in fuel cell. Perng and Wu [33] studied the angle and the height of trapezoid baffle on the net power. Bao and Bessler [34] performed a 2-D model to analyze the impact of long flow channel on polarization curve of the fuel cells.

The researches on PEM fuel cells can be generally divided into following categories according to the assumptions, accuracy of simulations, considered parameter and etc: one-, two-, or three-dimensional simulations, steady-state or transient behavior, isothermal or variable temperature, single- or two-phase, flow direction, channel configuration, size and properties of different sections, water uptake and management, thermal management, and performance optimization.

Scaling and similarity are important topics in mechanical engineering. The impacts of geometric scaling on the polarization curves of a device and circumstances in which the similarity occurs in some parameters are the questions at those topics. The answer to such questions has always been helpful in an analysis, prediction and experimentation of device's operation especially when the costs of experiment or times of analysis are too high. Due to the complexities of the processes, the scaling and similarity in fuel cells are questionable and interesting and have not been addressed yet. Therefore, they are considered here specifically.

2. Governing Equations, Assumptions and Numerical Procedure

In this study, the two-dimensional proton exchange membrane fuel cell is considered which is schematically shown in Fig. 1.

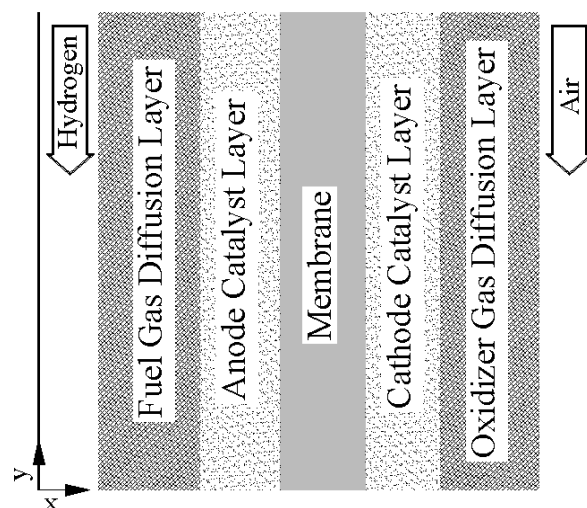


Fig. 1: Schematic configuration of problem.

The flow field is assumed to be single-phase, steady-state, and isothermal. The governing equations of the multi-component system are presented here:

$$\frac{\partial(L + L_v)}{\partial x} + \frac{\partial(G + G_v)}{\partial y} = ST \quad (1)$$

here:

$$L = \begin{bmatrix} \rho u \\ \rho u u + p \\ \rho u v \\ \rho u h \\ \rho u m_j \end{bmatrix} \quad G = \begin{bmatrix} \rho v \\ \rho v u \\ \rho v v + p \\ \rho v h \\ \rho v m_j \end{bmatrix} \quad L_v = \begin{bmatrix} 0 \\ -\tau_{xx} \\ -\tau_{xy} \\ -u\tau_{xx} - v\tau_{xy} \\ -\rho D_{eff} m_{j_x} \end{bmatrix} \quad G_v = \begin{bmatrix} 0 \\ -\tau_{yx} \\ -\tau_{yy} \\ -u\tau_{yx} - v\tau_{yy} \\ -\rho D_{eff} m_{j_y} \end{bmatrix} \quad ST = \begin{bmatrix} \sum \dot{\omega}_j \\ 0 \\ 0 \\ 0 \\ \dot{\omega}_j \end{bmatrix} \quad (2)$$

Where

$$D_{eff} = D \varepsilon^{1.5} \quad (3)$$

There are four species in the flow field which their mass rates of change are defined as:

$$\dot{\omega}_{H_2} = -\frac{2j_A}{2F} \quad \dot{\omega}_{O_2} = \frac{32j_C}{4F} \quad \dot{\omega}_{N_2} = 0 \quad \dot{\omega}_{H_2O} = -\frac{18j_C}{2F} \quad (4)$$

The exchange current densities are calculated by the following equations:

$$j_A = j_{Aref} \left(\frac{c_{H_2}}{c_{H_2ref}} \right)^{r_a} \left[\exp\left(\frac{\alpha_{A,A} F \eta_A}{RT} \right) - \exp\left(-\frac{\alpha_{A,C} F \eta_A}{RT} \right) \right] \quad (5)$$

$$j_C = j_{Cref} \left(\frac{c_{O_2}}{c_{O_2ref}} \right)^{r_c} \left[\exp\left(\frac{\alpha_{C,A} F \eta_C}{RT} \right) - \exp\left(-\frac{\alpha_{C,C} F \eta_C}{RT} \right) \right]$$

The over-potentials are defined as:

$$\eta_A = \phi_e - \phi_p \quad (6)$$

$$\eta_C = \phi_e - \phi_p - U_o$$

where [32]

$$U_o = 1.23 - 9 \times 10^{-4} (T - 298) \quad (7)$$

Besides the flow field equations, the equations for electric and ionic potentials are:

$$\nabla \cdot (-\sigma \nabla \phi_e) = S_e \quad (8)$$

$$\nabla \cdot (-\kappa \nabla \phi_p) = S_p$$

here:

$$S_e = \begin{cases} -j_A & \text{at Anode} \\ -j_C & \text{at Cathode} \end{cases} \quad (9)$$

$$S_p = \begin{cases} j_A & \text{at Anode} \\ j_C & \text{at Cathode} \end{cases}$$

The ionic potential equation is solved in the catalyst layers and the membrane, but the electric potential equation is solved in the catalyst layers and the gas diffusion layers (GDL). Total current density of the fuel cell is computed by integrating the exchange current densities on anode or cathode catalyst layers:

$$I \times L_c = \iint_{anode} |j_A| dA = \iint_{cathode} |j_C| dA \quad (10)$$

For numerical computation, the cell-centered finite-volume method is used. Viscous terms are treated using a central scheme and inviscid terms are treated using an AUSM⁺ method. The gradients are computed here in standard finite volume manner by using the Green's theorem.

The simulation procedure has been validated using various problems, and it has also been utilized to study different flows where details can be found in references [35-39]. The velocities and mass fractions of the species are specified as a boundary condition for inflow streams. The zero electric potential is applied on the interface of fuel channel and GDL (anode side), and the cell's working voltage is applied on the interface of oxidizer channel and GDL (cathode side) for electric potential equation. Zero-flux boundary condition is applied on the interfaces of GDL and catalyst layer at both anode and cathode sides for ionic potential equation.

3. Results and Discussion

To investigate the problem under consideration, at first the influence of the distribution of an oxygen concentration inside the PEMFC is studied on its polarization curve. The geometric and physical parameters adopted in the present paper are introduced in Table 1. After the grid independency study, the mesh resolution of 105×60 is used in simulations. The polarization curve is shown in Fig. 2. The left sharp drop in this curve corresponds to the activation polarization, and the right sharp drop corresponds to the concentration polarization.

The region of concentration polarization (mass transport limitation region) depends on the ability of oxygen molecules to diffuse through the oxidizer gas diffusion layer to the cathode catalyst layer. At high electric currents and especially when the inlet oxygen is diluted, the oxygen concentration in the catalyst layer (CL) is very low and the oxygen is almost entirely consumed at the GDL-CL interface, so the rate of the reaction that consumes the electrons cannot increase anymore, and concentration polarization region appears in the polarization curve. The actual limiting current density of this PEMFC is about 11.4 kA m⁻².

Table 1: Geometric and physical parameters of the FC

Quantity	Value
Fuel channel thickness (m)	1.e-4
Fuel gas diffusion layer thickness (m)	1.e-4
Anode catalyst layer thickness (m)	4.e-5
Membrane thickness (m)	1.e-4
Cathode catalyst layer thickness (m)	4.e-5
Oxidizer gas diffusion layer thickness (m)	1.e-4
Oxidizer channel thickness (m)	1.e-4
Channel length (m)	6.e-2
Fuel gas diffusion layer porosity	0.4
Anode catalyst layer porosity	0.1
Cathode catalyst layer porosity	0.1
Oxidizer gas diffusion layer porosity	0.4
Electric conductivity of fuel gas diffusion layer (Sm^{-1})	1.e3
Electric conductivity of anode catalyst layer (Sm^{-1})	1.5e3
Electric conductivity of cathode catalyst layer (Sm^{-1})	2.e3
Electric conductivity of oxidizer gas diffusion layer (Sm^{-1})	3.e3
Ionic conductivity of anode catalyst layer (Sm^{-1})	3.
Ionic conductivity of membrane (Sm^{-1})	5.
Ionic conductivity of cathode catalyst layer (Sm^{-1})	10.
Anode reference exchange current density (Am^{-3})	9.e8
Cathode reference exchange current density (Am^{-3})	250.
Hydrogen concentration power	1
Oxygen concentration power	1
Hydrogen reference concentration (k mole m^{-3})	40.e-3
Oxygen reference concentration (k mole m^{-3})	40.e-3
Charge transfer coefficients	1.
Working temperature (K)	353.
Inlet pressures (bar)	1.
Inlet velocities (ms^{-1})	5.
Oxygen mass fraction at oxidizer stream	0.2

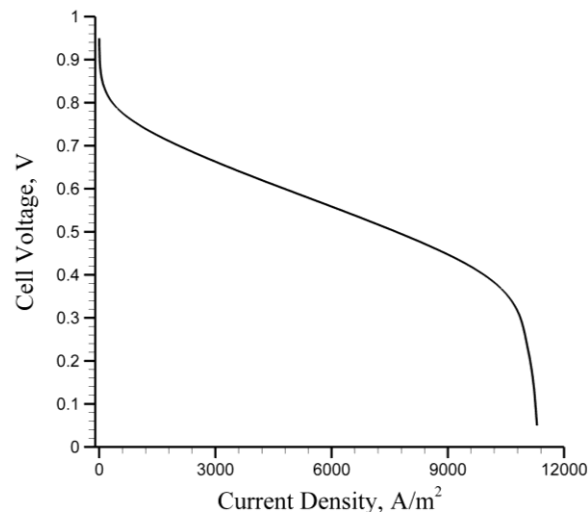


Fig. 2: Polarization curve of FC.

To emphasize the importance of the concentration term of the Butler-Volmer equation (eq. 5), the polarization curve is reproduced in two other different situations: first the concentration is kept

constant and equal to the inlet value, then the channel length is reduced to one-percent of the original length. The results are illustrated in Fig. 3. In an unrealistic situation of constant concentration, the maximum current density has increased to 29 kA m^{-2} which is about three times the actual value. In the short-channel situation, although the impacts of longitudinal variation of species concentration (along channel) are eliminated, the concentrations vary across the channel. So even though there is no mass transport limitation region in the polarization curve, the concentration affects the behavior of the PEMFC and decreases the maximum available current density even for short channel lengths.

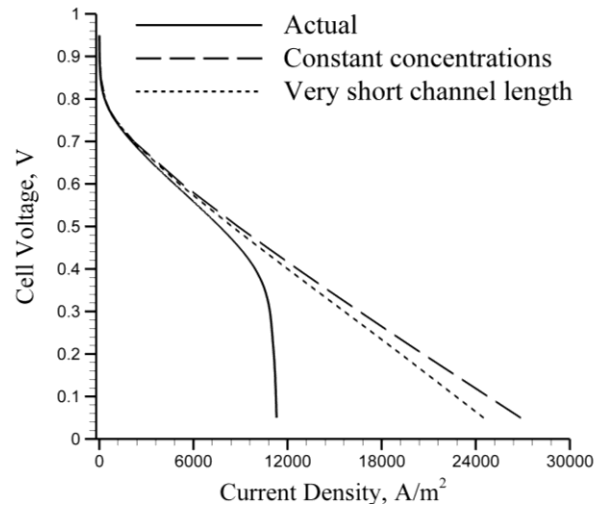


Fig. 3: Polarization curves in different situations.

Variations of oxygen concentration along the interface of cathode catalyst layer and oxidizer gas diffusion layer are presented for different working potentials in Fig. 4. This figure demonstrates the oxygen deterioration especially for low voltages (high electric currents) that leads to the mass transport limiting behavior. In addition, oxygen concentration variation across the CL and GDL is shown in Fig. 5 to affirm the concentration effects at high currents even in short-channel PEMFCs.

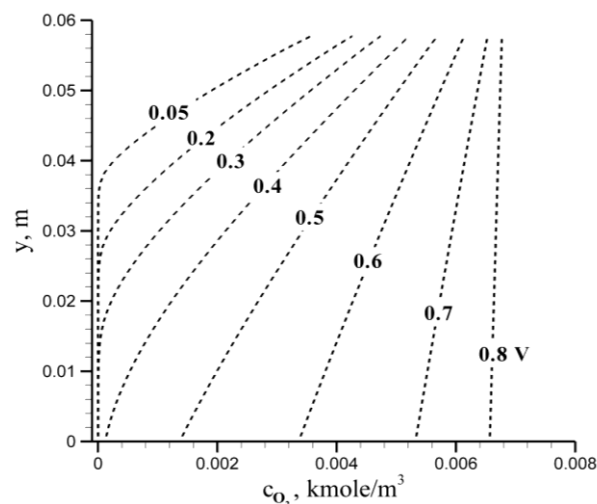


Fig. 4: Oxygen concentration along the CL-GDL interface for different working potentials.

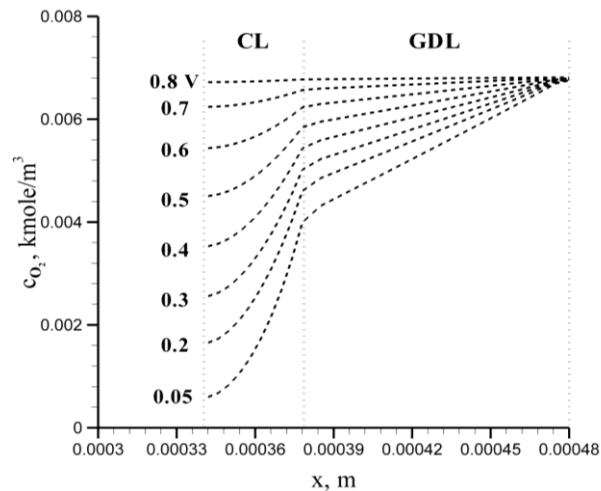


Fig. 5: Oxygen concentration across the CL-GDL for different working potentials of the short-channel FC.

Performance of the PEMFCs is an outcome of the interactions between the flow field equations and the electric and ionic potential equations. Although a main section of the polarization curve is almost linear, there are two other important regions which the mass transport region is quite dependent to the flow field's behavior that determines the limiting current density of the FC. With regards to the mentioned complexities, the existence of the similarity in the PEMFCs is examined here.

According to the physics of the governing equations, the results show that by scaling the fuel cell's geometry using the scale factor of sc , there can be similar behavior for the PEMFC if the velocity is multiplied by sc and the diffusion coefficients (D, μ, κ, σ) are multiplied by sc^2 . In this case, the flow field and potential fields are similar and the current density is multiplied by sc . So the polarization curve is exactly similar in whole regions. By applying the scale factor of 0.5, the polarization curves are compared in Fig. 6. In addition, the profiles of the oxygen concentration and the ionic potential for the working voltage of 0.2 are illustrated in Figs. 7-9 which demonstrate the similarity of the flow and potential fields too. The similarity may help a lot in numerical and experimental studies on this complicated device.

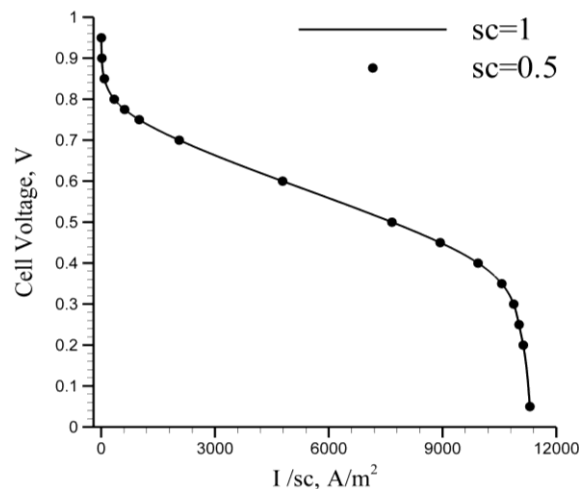


Fig. 6: Similarity of the polarization curves.

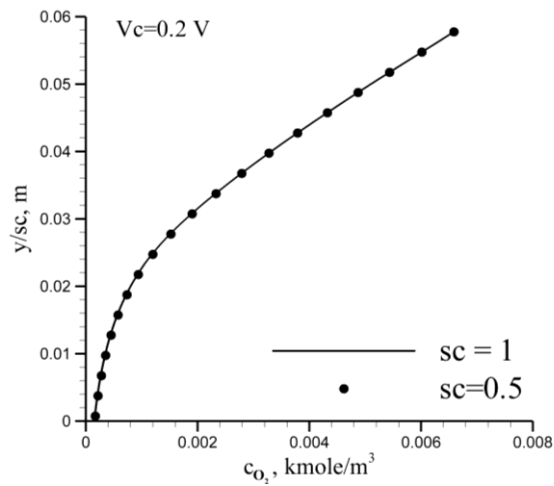


Fig. 7: Similarity of concentration profiles along the channel external wall ($x=X_{max}$).

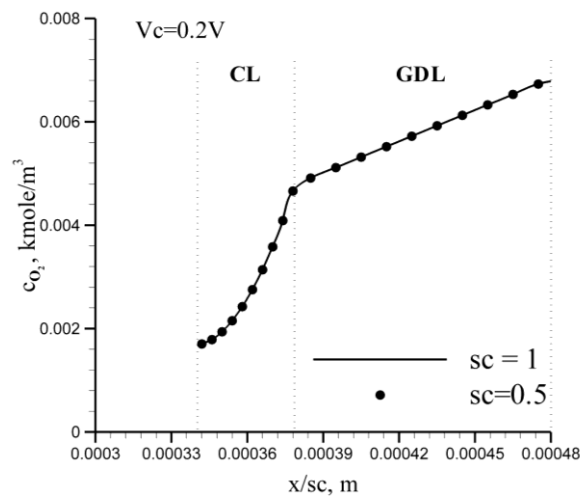


Fig. 8: Similarity of concentration profiles across the CL-GDL at $y=L_c$.

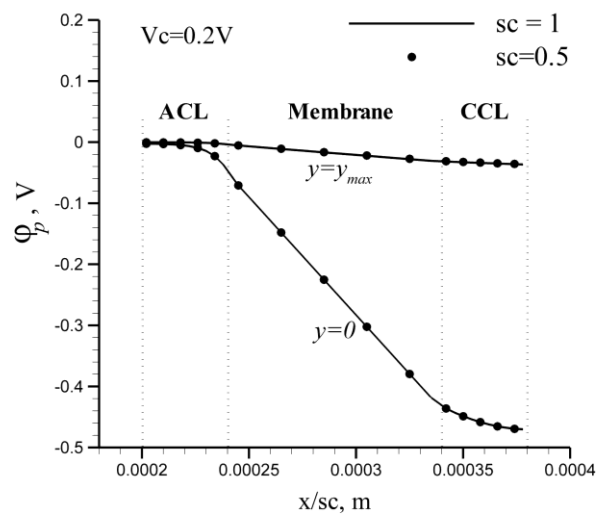


Fig. 9: Similarity of the potential fields.

As mentioned, by scaling the geometry of the fuel cell, it is possible to change properly some parameters to have similar behavior. Here, the question is what if the geometry is just scaled keeping the same parameters? To investigate the impacts of geometric scaling, the considered PEMFC is scaled-up once and scaled-down again and the polarization curves are computed where are shown in Fig. 10.

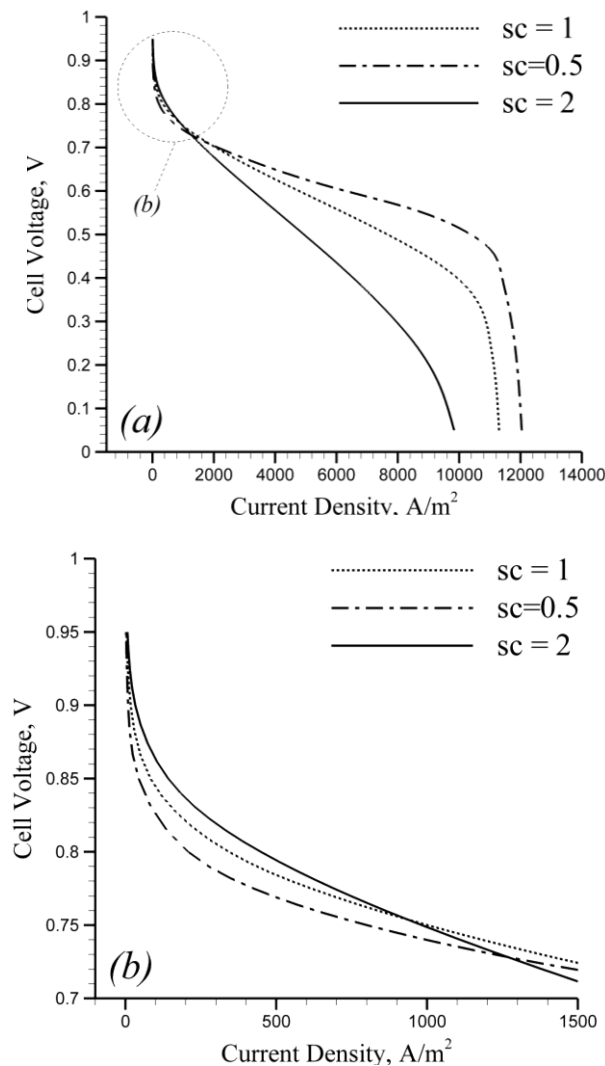


Fig. 10: Polarization curves for different geometric scaling, a) whole regions, b) activation region.

The results illustrate that the geometric-scaling of the fuel cell has different impacts on the regions of the polarization curve. Scaling-up the fuel cell increases the current density in the activation region and decreases it in other regions, but the effect of scaling-down is opposite; it decreases the current density in the activation regions and increases the current in other regions. In addition, the concentration polarization region is magnified by scaling-down the fuel cells. This is interesting because although the scale-down reduces the channel length and one may guess at a first glance that it attenuates the concentration effect, but this is not true and the effect of geometric change in cross-direction is dominant and the mass transport limiting region is amplified in this situation.

4. Conclusions

Numerical studies of the proton exchange membrane fuel cells are performed here using the two-dimensional, single-phase, steady-state, isothermal, and multi-component system of equations. The effects of the distribution of oxygen concentration is investigated on the polarization curve and it is illustrated that it is an important parameter on the fuel cell behavior and for determining the maximum current density even in short-channel fuel cells. The similarity of the fuel cells is investigated and it is concluded that using proper way to change the required parameters, similar behavior can be found by scaling the fuel cells. Using the geometric scale factor of sc , there can be the similarity in the PEMFC if the velocity is multiplied by sc and the diffusion coefficients are multiplied by sc^2 . In this case, the flow and potential fields are similar and the current density is multiplied by sc and the polarization curve is exactly similar in all regions. In addition, the impacts of geometric-scaling are studied and it is concluded that it affects the regions of the polarization curve differently, and scaling-down the fuel cell amplifies the mass transport limiting region, unexpectedly.

References

- [1] V. Gurau, H. Liu, and S. Kakac, Two-Dimensional Model for Proton Exchange Membrane Fuel Cells, *AIChE Journal*, vol 44 , pp. 2410-2422, 1998.
- [2] D. Singh, D. Lu, and N. Djilali, A Two-Dimensional Analysis of Mass Transport in Proton Exchange Membrane Fuel Cells, *International Journal of Engineering Science*, vol 37, pp. 431-452, 1999.
- [3] S. Dutta, S. Shimpalee, and J. Van Zee, Three-Dimensional Numerical Simulation of Straight Channel PEM Fuel Cells, *Journal of Applied Electrochemistry*, vol 30, pp. 135-146, 2000.
- [4] S. Shimpalee, and S. Dutta, Numerical Prediction of Temperature Distribution in PEM Fuel Cells, *Numerical Heat Transfer*, vol 38, pp. 111-128, 2000.
- [5] I. Hsing, and P. Futerko, Two-Dimensional Simulation of Water Transport in Polymer Electrolyte Fuel Cells, *Chemical Engineering Science*, vol 55, pp. 4209-4218, 2000.
- [6] D. Natarajan, and T. Nguyen, A Two-Dimensional, Two-Phase, Multi-Component, Transient Model for the Cathode of a Proton Exchange Membrane Fuel Cell Using Conventional Gas Distributors, *Journal of Electrochemical Society*, vol 148, pp. 1324-1335, 2001.
- [7] Z. Wang, C. Wang, and K. Chen, Two-Phase Flow and Transport in the Air Cathode of Proton Exchange Membrane Fuel Cells, *Journal of Power Sources*, vol 94, pp. 40-50, 2001.
- [8] L. Youand, and H. Liu, A Two-Phase Flow and Transport Model for the Cathode of PEM Fuel Cells, *International Journal of Heat and Mass Transfer*, vol 45, pp. 2277-2287, 2002.
- [9] H. Chu, C. Yeh, and F. Chen, Effects of Porosity Change of Gas Diffuser on Performance of Proton Exchange Membrane Fuel Cell, *Journal of Power Sources*, vol 123, pp. 1-9, 2003.
- [10] T. Berning, and N. Djilali, Three-Dimensional Computational Analysis of Transport Phenomena in a PEM Fuel Cell—a Parametric Study, *Journal of Power Sources*, vol 124, pp. 440-452, 2003.
- [11] P. Nguyen, T. Berning, and N. Djilali, Computational Model of a PEM Fuel Cell with Serpentine Gas Flow Channels, *Journal of Power Sources*, vol 130, pp. 149-157, 2004.
- [12] M. Hu, X. Zhu, M. Wang, A. Gu, and L. Yu, Three Dimensional, Two Phase Flow Mathematical Model for PEM Fuel Cell, *Energy Conversion and Management*, vol 45, pp. 1861-1916, 2004.

- [13] G. Hu, J. Fan, S. Chen, Y. Liu, and K. Cen, Three-Dimensional Numerical Analysis of Proton Exchange Membrane Fuel Cells with Conventional and Interdigitated Flow Fields, *Journal of Power Sources*, vol 136, pp. 1-9, 2004.
- [14] K. Lum, and J. McGuirk, Three-Dimensional Model of a Complete Polymer Electrolyte Membrane Fuel Cell–Model Formulation, Validation and Parametric Studies, *Journal of Power Sources*, vol 143, pp. 103-124, 2005.
- [15] W. Ying, T. Yang, W. Lee, J. Ke, and C. Kim, Three-Dimensional Analysis for Effect of Channel Configuration on the Performance of a Small Air-Breathing Proton Exchange Membrane Fuel Cell, *Journal of Power Sources*, vol 145, pp. 572-581, 2005.
- [16] G. Inoue, Y. Matsukuma, and M. Minemoto, Effect of Gas Channel Depth on Current Density Distribution of Polymer Electrolyte Fuel Cell by Numerical Analysis Including Gas Flow through Gas Diffusion Layer, *Journal of Power Sources*, vol 157, pp. 136-152, 2006.
- [17] H. Lin, C. Cheng, C. Soong, F. Chen, and W. Yan, Optimization of Key Parameters in the Proton Exchange Membrane Fuel Cell, *Journal of Power Sources*, vol 162, pp. 246-254, 2006.
- [18] W. Yan, H. Liu, C. Soong, F. Chen, and C. Cheng, Numerical Study on Cell Performance and Local Transport Phenomena of PEM Fuel Cells with Novel Flow Field Designs, *Journal of Power Sources*, vol 161, pp. 907-919, 2006.
- [19] H. Meng, A Three-Dimensional Mixed-Domain PEM Fuel Cell Model with Fully-Coupled Transport Phenomena, *Journal of Power Sources*, vol 164, pp. 688-696, 2007.
- [20] H. Meng, A Two-Phase Non-Isothermal Mixed-Domain PEM Fuel Cell Model and its Application to Two-Dimensional Simulations, *Journal of Power Sources*, vol 168, pp. 218-228, 2007.
- [21] H. Meng, Numerical Investigation of Transient Responses of a PEM Fuel Cell Using a Two-Phase Non-Isothermal Mixed-Domain Model, *Journal of Power Sources*, vol 171, pp. 738-746, 2007.
- [22] M. Secanell, B. Carnes, A. Suleman, and N. Djilali, Numerical Optimization of Proton Exchange Membrane Fuel Cell Cathodes, *Electrochimica ACTA*, vol 52, pp. 2668-2682, 2007.
- [23] S. Shimpalee, and J. Van Zee, Numerical Studies on Rib & Channel Dimension of Flow-Field on PEMFC Performance, *International Journal of Hydrogen Energy*, vol 32, pp. 842-856, 2007.
- [24] C. Cheng, H. Lin, and G. Lai, Numerical Prediction of the Effect of Catalyst Layer Nafion Loading on the Performance of PEM Fuel Cells, *Journal of Power Sources*, vol 164, pp. 730-741, 2007.
- [25] H. Wu, X. Li, and P. Berg, Numerical Analysis of Dynamic Processes in Fully Humidified PEM Fuel Cells, *International Journal of Hydrogen Energy*, vol 32, pp. 2022-2031, 2007.
- [26] Jang, J., Yan, W., Li, H., and Tsai, W., Three-Dimensional Numerical Study on Cell Performance and Transport Phenomena of PEM Fuel Cells with Conventional Flowfields, *International Journal of Hydrogen Energy*, vol 33, pp. 156-164, 2008.
- [27] V. Gurau, and J. Mann, A Critical Overview of Computational Fluid Dynamics Multiphase Models for Proton Exchange Membrane Fuel Cells, *SIAM Journal of Applied Mathematics*, vol 70, pp. 410-454, 2009.
- [28] C. Min, A Novel Three-Dimensional, Two-Phase and Non-Isothermal Numerical Model for Proton Exchange Membrane Fuel Cell, *Journal of Power Sources*, vol 195, pp. 1880-1887, 2010.
- [29] E. Fontana, E. Mancusi, and A. Silva, Study of the Effects of Flow Channel with Non-Uniform Cross-Sectional Area on PEMFC Species and Heat Transfer, *International Journal of Heat and Mass Transfer*, vol 54, pp. 4462-4472, 2011.

- [30] P. Massonnat, F. Gao, R. Roche, D. Paire, D. Bouquain, and A. Miraoui, Multiphysical, Multidimensional Real-Time PEM Fuel Cell Modeling for Embedded Applications, *Energy Conversion and Management*, vol 88, pp. 554-564, 2014.
- [31] E. Mancusi, E. Fontana, and A. Souza, Numerical Study of Two-Phase Flow Patterns in the Gas Channel of PEM Fuel Cells with Tapered Flow Field Design, *International Journal of Hydrogen Energy*, vol 39, pp. 2261-2273, 2014.
- [32] S. Chaudhary, V. Sachan, and P. Bhattacharya, Two Dimensional Modelling of Water Uptake in Proton Exchange Membrane Fuel Cell, *International Journal of Hydrogen Energy*, vol 39, pp. 17802-17818, 2014.
- [33] S. Perng, and H. Wu, A Three-Dimensional Numerical Investigation of Trapezoid Baffles Effect on Non-Isothermal Reactant Transport and Cell Net Power in a PEMFC, *Applied Energy*, vol 143, pp. 81-95, 2015.
- [34] C. Bao, and W. Bessler, Two-Dimensional Modeling of a Polymer Electrolyte Membrane Fuel Cell with Long Fow Channel. Part I. Model Development, *Journal of Power Sources*, vol 275, pp. 922-934, 2015.
- [35] A. M. Tahsini, The Influence of an Optical Cavity's Diamond Pattern on the Performance of the Gas Dynamic Lasers, accepted for publication, *The Aeronautical Journal*, vol 120, pp. 1932-1942, 2016.
- [36] A. M. Tahsini, Detonation Wave Attenuation in Dust-Free and Dusty Air, *Journal of Loss Prevention in the Process Industries*, vol 39, pp. 24-29, 2016.
- [37] A. M. Tahsini, and S. Tadayon Mousavi, Investigating the Supersonic Combustion Efficiency for the Jet-in-Cross-Flow, *International Journal of Hydrogen Energy*, vol 40, pp. 3091-3097, 2015.
- [38] A. M. Tahsini, Heat Release Effects on Drag Reduction in High Speed Flows, *International Journal of Heat and Mass Transfer*, vol 57, pp. 657-661, 2013.
- [39] A. M. Tahsini, and M. Farshchi, Numerical Study of Solid Fuel Evaporation and Auto-Ignition in a Dump Combustor, *ACTA Astronautica*, vol 67, pp. 774-783, 2010.